

CrossMark
click for updatesCite this: *Chem. Sci.*, 2016, 7, 4052

Catalytic radical reduction in aqueous solution via oxidation of biologically-relevant alcohols†

Yamin Htet^a and Andrew G. Tennyson^{*abc}

Metalloenzymes that normally perform catalytic antioxidant or radical-degrading functions, as well as small-molecule complexes that mimic them, can also exert pro-oxidant or radical-forming effects depending on the identity of the terminal reductant. Because nitroxyl radicals function as redox active cocatalysts in the aerobic oxidation of alcohols, we hypothesized that catalytic radical reduction could be achieved via the oxidation of biologically-relevant alcohols. Herein we report an organoruthenium complex (**Ru1**) that catalyzed reduction of 2,2'-azino-bis(3-ethylbenzo-thiazoline-6-sulfonate) radical monoanion (ABTS^{•-}) to ABTS²⁻ in phosphate buffered saline (pH 7.4) using MeOH, EtOH, i-PrOH, serine, threonine, glucose, arabinose, methyl lactate or dimethyl malate as the terminal reductant. Replacing either the C-H or O-H groups of a -CHOH- moiety resulted in the loss of ABTS^{•-} reducing ability. Moreover, in conjunction with an alcohol terminal reductant, **Ru1** was able to inhibit the oxidation of ABTS²⁻ by H₂O₂ and horseradish peroxidase, even after multiple successive challenges with excess H₂O₂ or ABTS^{•-}. Collectively, these results demonstrate that **Ru1** inhibits the oxidative formation of and catalyzes the reduction of radicals in aqueous solution via oxidation of biologically-relevant alcohols.

Received 12th February 2016

Accepted 4th March 2016

DOI: 10.1039/c6sc00651e

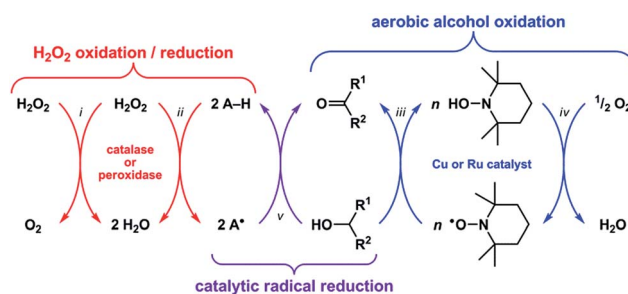
www.rsc.org/chemicalscience

Introduction

Reactive oxygen species (ROS) such as superoxide (O₂⁻) and hydrogen peroxide (H₂O₂) can alter the structures and functions of biomolecules^{1,2} via DNA base lesion formation,³ transition metal ion release from proteins,⁴ and membrane phospholipid chain degradation.⁵ Antioxidants can prevent or attenuate this damage by reacting with ROS to yield less oxidizing, more stable radical or non-radical products. Superoxide dismutase (SOD) and catalase, for example, are metalloenzymes that protect cells by catalyzing the disproportionation of O₂⁻ and H₂O₂, respectively.⁶ Synthetic Mn-salen and Mn-porphyrin complexes have demonstrated both SOD and catalase activity,⁷ and some have entered phase 1 clinical trials as therapeutics for neurodegenerative and pulmonary diseases.⁸

Recent studies have shown that these classes of synthetic Mn complexes can also exert pro-oxidant effects at low ROS concentrations,^{9,10} dichotomous behavior that is consistent with the enzymes they mimic. Catalase converts 2H₂O₂ into O₂ + 2H₂O (Scheme 1-i),¹¹ wherein the first equivalent of H₂O₂ is reduced to H₂O and generates an Fe(IV)=O⁺ intermediate,

which then oxidizes the second equivalent of H₂O₂ to O₂ and releases H₂O.¹² At low H₂O₂ concentrations, this Fe(IV)=O⁺ intermediate can abstract H[•] from other molecules (*i.e.*, A-H) and thus exhibit peroxidase-like reactivity (Scheme 1-ii).¹³ Conversely, peroxidase can exhibit catalase-like reactivity at low A-H/high H₂O₂ concentrations.¹⁴ Because the Mn-salen and Mn-porphyrin complexes proceed through high-valent Mn oxo/hydroxo intermediates¹⁵⁻¹⁸ with oxidizing power comparable to Fe(IV)=O⁺, their reactivity will mimic catalase or peroxidase based on the availability of H₂O₂. Therefore, the function of catalase and its biomimetic Mn complexes as either



Scheme 1 Catalase normally catalyzes the disproportionation of 2H₂O₂ → O₂ + 2H₂O (i), but at low H₂O₂ concentrations it can abstract H[•] from other molecules (A-H) and produce radicals (A[•]) in a manner similar to peroxidase (ii). Copper or ruthenium complexes can catalyze the oxidation of R¹-CHOH-R² to R¹-C(=O)-R² using a nitroxyl radical (*e.g.*, TEMPO, *n* = 1 for Cu, *n* = 2 for Ru) as the H[•] abstracting reagent (iii) and O₂ as the terminal oxidant (iv). By a similar mechanism, a complex could catalyze radical reduction using a biologically relevant non-tertiary alcohol as the terminal reductant (v).

^aDepartment of Chemistry, Clemson University, Clemson, SC 29634, USA. E-mail: atennys@clemson.edu

^bDepartment of Materials Science and Engineering, Clemson University, Clemson, SC 29634, USA

^cCenter for Optical Materials Science and Engineering Technologies, Anderson, SC 29625, USA

† Electronic supplementary information (ESI) available. See DOI: 10.1039/c6sc00651e



antioxidants or pro-oxidants will be determined by the nature of the terminal reductant.

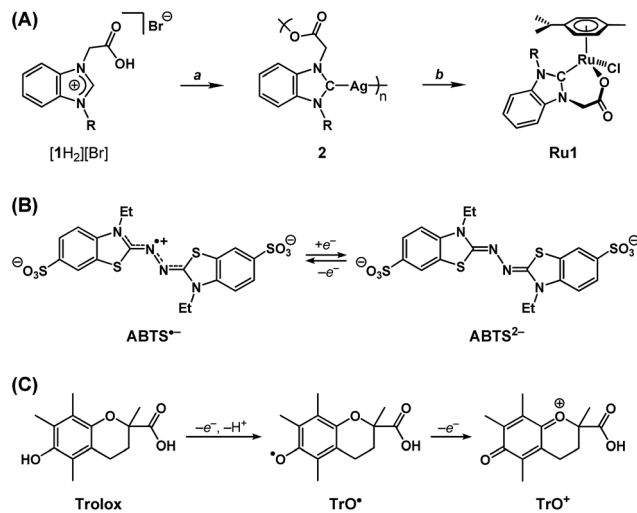
A catalytic oxidation reaction important in synthetic chemistry is the aerobic oxidation of $R^1\text{-CHOH-R}^2$ to $R^1\text{-C(=O)-R}^2$ that does not cause any (1) over-oxidation to $R\text{-COOH}$ or (2) undesired reactions at other functional groups.^{19–23} One strategy employs a copper or ruthenium catalyst in conjunction with a nitroxyl radical, such as 2,2,6,6-tetramethylpiperidinyl-*N*-oxyl (TEMPO), to oxidize $R^1\text{-CHOH-R}^2$ to $R^1\text{-C(=O)-R}^2$ with concomitant formation of TEMPO-H (Scheme 1-iii). Subsequent regeneration of the TEMPO radical occurs with the oxidation of TEMPO-H by O_2 , which functions as the terminal oxidant for this reaction (Scheme 1-iv). Because the TEMPO radical is reduced by $R^1\text{-CHOH-R}^2$ in the aerobic alcohol oxidation catalytic cycle, we hypothesized that the catalytic reduction of other radicals could also be achieved *via* the oxidation (*i.e.*, dehydrogenation) of non-tertiary alcohols (Scheme 1-v). Herein we report the validation of this hypothesis with an organoruthenium complex that catalyzes the reduction and inhibits the formation of radicals in buffered aqueous solutions *via* the oxidation of biologically-relevant non-tertiary alcohols. Given the successes of group 8 transfer hydrogenation catalysts as chemotherapeutics^{24,25} in particular and the burgeoning scope of medicinal applications for transition metal-based catalytic systems^{26–28} in general, we anticipate that the reduction of radicals *via* the Ru-catalyzed oxidation of alcohols will lead to new strategies for protecting against ROS *in vivo*.

Results and discussion

Approach and rationale

We recently reported a Ru complex supported by a chelating N-heterocyclic carbene-carboxylate ligand (**Ru1**, Scheme 2A) that catalyzed the hydrogenation of C=O, C=N and C=C bonds, in which the H_2 transferred was obtained from the oxidation of *i*-PrOH to acetone.²⁹ Based on this catalytic chemical reactivity observed with **Ru1** and previous reports of other Ru complexes with chelating carboxylate ligands exerting antioxidant effects in cells, which derived from irreversible stoichiometric reactions with nitric oxide,^{30,31} we hypothesized that **Ru1** would function as a catalytic antioxidant, reducing radicals using non-tertiary alcohols as terminal reductants. Using methods previously reported by our group,^{29,32} the N-heterocyclic carbene (NHC) ligand precursor $[1H_2][Br]$ was treated with Ag_2O to afford the Ag-NHC complex $[Ag(1)]_n$ (**2**). The NHC ligand was subsequently transferred to Ru *via* the reaction of **2** with $\{[RuCl(\eta^6\text{-cymene})]_2(\mu\text{-Cl})_2\}$, which yielded the Ru-NHC complex $[RuCl(1)(\eta^6\text{-cymene})]$ (**Ru1**).

As a radical substrate to probe antioxidant activity, 2,2'-azino-bis(3-ethylbenzothiazoline-6-sulfonate) radical monoanion ($ABTS^{\cdot-}$, Scheme 2B) was selected on the basis of its large extinction coefficient (ϵ) at long wavelengths ($\epsilon_{750} = 1.6 \times 10^4 \text{ M}^{-1} \text{ cm}^{-1}$ in EtOH and $\epsilon_{734} = 1.5 \times 10^4 \text{ M}^{-1} \text{ cm}^{-1}$ in aqueous buffer),³³ its reversible one-electron reduction to $ABTS^{2-}$ ($E_{1/2} = 0.68 \text{ V vs. NHE}$) falling within the range of potentials accessible in biological systems (-0.4 to $+0.8 \text{ V vs. NHE}$),³⁴ and its stability in aerobic, protic media. The longer absorption wavelength and



Scheme 2 (A) Synthesis of $[1H_2][Br]$, **2** and **Ru1**. Reagents and conditions: (a) Ag_2O (1.5 equiv.) or (b) $\{[RuCl(\eta^6\text{-cymene})]_2(\mu\text{-Cl})_2\}$ (1 : 1 Ag/Ru), CH_2Cl_2 , room temperature, 24 h. R = *p*-tolyl. (B) One-electron redox interconversion between $ABTS^{\cdot-}$ and $ABTS^{2-}$ (NH_4^+ counterions omitted for clarity). (C) First and second one-electron oxidations of Trolox.

greater extinction coefficient for $ABTS^{\cdot-}$ enables spectroscopic analysis of radical-degrading and -forming reactions (1) with less interference from other optically absorbing species present in biological systems and (2) at lower concentrations‡ more relevant to oxidative stress than would be possible with direct measurements of $O_2^{\cdot-}$ ($\epsilon_{250} = 1.9 \times 10^3 \text{ M}^{-1} \text{ cm}^{-1}$) or H_2O_2 ($\epsilon_{240} = 43.6 \text{ M}^{-1} \text{ cm}^{-1}$).^{35,36} Furthermore, the $1e^-$ reduction potential for $ABTS^{\cdot-}$ is lower than or comparable to the standard reduction potentials for several of the oxidizing species associated with oxidative stress in biological systems (*e.g.*, $E^\circ = 1.78 \text{ V}$ for H_2O_2 , 1.6 V for RO^{\cdot} , 1.0 V for ROO^{\cdot} , 0.92 V for Cys-S $^{\cdot}$, 0.70 for O_2 , *etc.*),³⁴ therefore $ABTS^{\cdot-}$ is a reasonable substrate for approximating biologically-relevant oxidants.

As a non-catalytic antioxidant control, Trolox (Scheme 2C) was employed given its use as a benchmark in a variety of radical degradation and antioxidant studies.³⁷ Trolox can serve as a $1e^-$ or $2e^-$ reductant, whereby the first $1e^-$ oxidation is accompanied by rapid H^+ loss to form a phenoxyl radical (TrO^{\cdot}), which can then undergo a second $1e^-$ oxidation to form a phenoxonium cation (TrO^+). However, in methanol (MeOH) or ethanol (EtOH) solutions, these processes converge into a single $2e^-$ oxidation.³⁸ Subsequent hydrolysis of TrO^+ can then cleave the tertiary carbon-oxonium bond, which renders the $2e^-$ oxidation of Trolox irreversible.

Because ROS and other oxidants can cause damage to critical biomolecules, inhibiting the formation of these oxidizing species in biological systems can potentially prevent the onset of harmful pathologies.² As a model system, we selected the oxidation of $ABTS^{2-}$ to $ABTS^{\cdot-}$ by horseradish peroxidase (HRP) and H_2O_2 (*i.e.*, Scheme 1-ii).³⁹ However, before studying the ability of **Ru1** to inhibit $ABTS^{\cdot-}$ formation, it was first necessary to explore the fundamental reactivity of **Ru1** with $ABTS^{\cdot-}$ under controlled conditions and achieve the catalytic reduction of $ABTS^{\cdot-}$ to $ABTS^{2-}$ in buffered aqueous solution.



Catalytic radical reduction in EtOH

Addition of 5 μM **Ru1** (CH_3CN stock) to 50 μM $\text{ABTS}^{\cdot-}$ in EtOH caused a 100% decay in $\text{ABTS}^{\cdot-}$ concentration within 15 min (Fig. 1, red line), accompanied by the formation of 50 μM ABTS^{2-} (Fig. S1†), indicating the 1 : 1 conversion of $\text{ABTS}^{\cdot-}$ to ABTS^{2-} by **Ru1**. No $\text{ABTS}^{\cdot-}$ degradation occurred when CH_3CN alone was added (Fig. 1, dotted green line), indicating that **Ru1** was essential for the reduction of $\text{ABTS}^{\cdot-}$ to ABTS^{2-} and that CH_3CN did not impact $\text{ABTS}^{\cdot-}$ stability. No $\text{ABTS}^{\cdot-}$ formation was observed in an aerobic solution containing 5 μM **Ru1** and 50 μM ABTS^{2-} , indicating that **Ru1** does not oxidize ABTS^{2-} to $\text{ABTS}^{\cdot-}$ under these conditions. In contrast to **Ru1**, the addition of 5 μM Trolox caused a rapid (within mixing time) 22% decrease in $\text{ABTS}^{\cdot-}$ concentration (Fig. 1, blue line), which corresponded to the reduction of 10 μM $\text{ABTS}^{\cdot-}$ (2 equiv. *vs.* Trolox) and was consistent with the ability of Trolox to serve as a non-catalytic $2e^-$ reductant in EtOH solution.³⁸

To assess its catalytic potential and corresponding regeneration, the reactivity of **Ru1** with multiple sequential aliquots of excess $\text{ABTS}^{\cdot-}$ was examined. After the reduction of 50 μM $\text{ABTS}^{\cdot-}$ by 5 μM **Ru1** was complete (Fig. 2, red line), 2 additional 50 μM $\text{ABTS}^{\cdot-}$ aliquots were introduced and complete $\text{ABTS}^{\cdot-}$ reduction was observed in each instance, indicating that **Ru1** remained catalytically competent for the complete reduction of

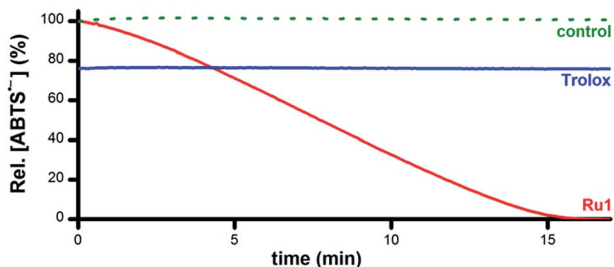


Fig. 1 Plot of relative $[\text{ABTS}^{\cdot-}]$ vs. time in EtOH following the addition of **Ru1** (CH_3CN stock, red line), Trolox (CH_3CN stock, blue line), or CH_3CN alone (dotted green line). Conditions: $[\text{Ru1}]_0$ or $[\text{Trolox}] = 5 \mu\text{M}$, $[\text{ABTS}^{\cdot-}]_0 = 50 \mu\text{M}$, EtOH, 25 $^\circ\text{C}$; $[\text{ABTS}^{\cdot-}]$ determined using absorbance measured at 750 nm and $\epsilon_{750} = 1.6 \times 10^4 \text{ M}^{-1} \text{ cm}^{-1}$ (ref. 33).

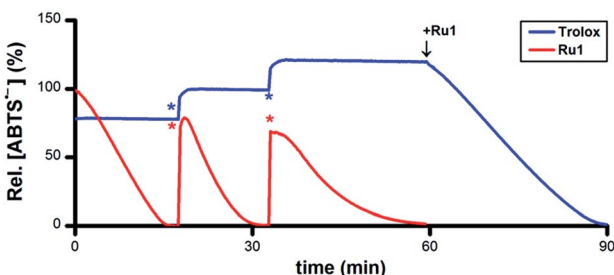


Fig. 2 Plot of relative $[\text{ABTS}^{\cdot-}]$ vs. time which shows the reduction of $\text{ABTS}^{\cdot-}$ after adding **Ru1** (red line) followed by 2 additional 50 μM $\text{ABTS}^{\cdot-}$ aliquots (*) and Trolox (blue line) followed by 2 additional 10 μM $\text{ABTS}^{\cdot-}$ aliquots (*), then 5 μM **Ru1**. Conditions: $[\text{Ru1}]_0$ or $[\text{Trolox}]_0 = 5 \mu\text{M}$, $[\text{ABTS}^{\cdot-}]_0 = 50 \mu\text{M}$, EtOH, 25 $^\circ\text{C}$; $[\text{ABTS}^{\cdot-}]$ determined using absorbance measured at 750 nm and $\epsilon_{750} = 1.6 \times 10^4 \text{ M}^{-1} \text{ cm}^{-1}$ (ref. 33).

150 μM $\text{ABTS}^{\cdot-}$ (30 turnovers). Unlike **Ru1**, the addition of successive 10 μM aliquots of $\text{ABTS}^{\cdot-}$ following the initial reduction by 5 μM Trolox (Fig. 2, blue line) only caused the radical absorbance to increase by amounts equivalent to the concentration of $\text{ABTS}^{\cdot-}$ added, indicating that the antioxidant capacity of Trolox had been exhausted after the reduction of only 2 equiv. of $\text{ABTS}^{\cdot-}$. However, subsequent addition of 5 μM **Ru1** to the exhausted Trolox solution containing 70 μM $\text{ABTS}^{\cdot-}$ resulted in 100% radical reduction within 30 min.

Addition of 5 μM ascorbate (AsCH^-) or 5 μM glutathione (GSH) to a solution of 50 μM $\text{ABTS}^{\cdot-}$ in EtOH caused the $\text{ABTS}^{\cdot-}$ concentration to decrease by 5% or 60% (Fig. S2 and S3†), values that were consistent with their ability to function as $1e^-$ or $6e^-$ reductants, respectively, under these experimental conditions.^{40–42} Similar to the experiments with Trolox, subsequent addition of $\text{ABTS}^{\cdot-}$ only afforded increases in radical absorbance equal to the concentration of $\text{ABTS}^{\cdot-}$ added, which likewise indicated that the antioxidant capacity of AsCH^- and GSH had been exhausted. Quantitative radical reduction could nonetheless be achieved *via* addition of 5 μM **Ru1** to the exhausted AsCH^- or GSH solutions that contained excess $\text{ABTS}^{\cdot-}$. Collectively, these data demonstrate that **Ru1** can catalytically reduce $\text{ABTS}^{\cdot-}$ and, because it is regenerated after each reaction cycle, that a catalytic antioxidant can offer significantly greater protection than traditional stoichiometric antioxidants, such as Trolox, AsCH^- and GSH.

Although $\text{ABTS}^{\cdot-}$ degradation has been previously observed with other Ru complexes,^{43–45} **Ru1** is the first to demonstrate catalytic $\text{ABTS}^{\cdot-}$ reduction. It is important to note that the previous studies measured percentage of $\text{ABTS}^{\cdot-}$ degradation with respect to Ru complex concentration, for the purpose of determining the dose dependence of radical degradation. However, the reported absorbance *vs.* time plots displayed significantly slower $\text{ABTS}^{\cdot-}$ degradation for the Ru complexes compared to Trolox (much like **Ru1** *vs.* Trolox, Fig. 1) and 100% $\text{ABTS}^{\cdot-}$ degradation at multiple Ru concentrations (demonstrating dose independence). Thus, it is possible that a previously reported Ru complex may have degraded $\text{ABTS}^{\cdot-}$ catalytically, but its significantly slower reactivity compared to Trolox created the appearance that the percent of $\text{ABTS}^{\cdot-}$ degraded was dependent on Ru complex concentration and led to the conclusion that the observed radical degradation was non-catalytic.

Catalytic radical reduction in aqueous buffer

As a catalyst for the $1e^-$ reduction of $\text{ABTS}^{\cdot-}$ to ABTS^{2-} , **Ru1** itself cannot serve as the terminal reductant for this reaction, a role most likely played by the EtOH solvent for the experiments displayed in Fig. 1. To test this hypothesis and identify the chemical features required for terminal reductant function, it was first necessary to determine experimental conditions under which no $\text{ABTS}^{\cdot-}$ degradation occurred in the presence of **Ru1** alone. Phosphate-buffered saline (PBS, pH 7.4) was selected as a suitable reaction medium because neither the solvent (H_2O) nor the buffer components (Na_2HPO_4 , KH_2PO_4 , NaCl , KCl) would undergo oxidation to supply the electrons necessary



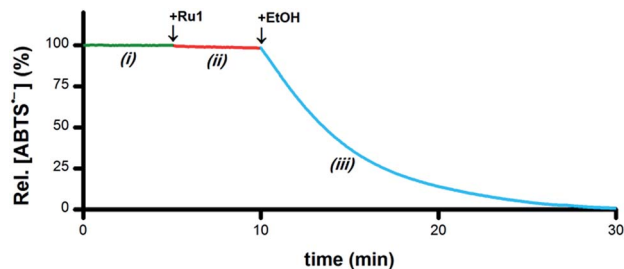


Fig. 3 Plot of relative $[\text{ABTS}^{\bullet-}]$ vs. time which shows the catalytic reduction of $\text{ABTS}^{\bullet-}$ by **Ru1** in PBS. By itself, $\text{ABTS}^{\bullet-}$ was stable in PBS (i, green line). Addition of **Ru1** did not cause $\text{ABTS}^{\bullet-}$ reduction (ii, red line). Subsequent addition of EtOH caused the absorbance to decrease (iii, blue line), which indicated that EtOH functioned as a terminal reductant. Conditions: $[\text{Ru1}]_0 = 5 \mu\text{M}$, $[\text{ABTS}^{\bullet-}]_0 = 50 \mu\text{M}$, $[\text{EtOH}]_0 = 50 \text{mM}$, PBS (pH 7.4), 25°C ; $[\text{ABTS}^{\bullet-}]$ determined using absorbance measured at 734 nm and $\epsilon_{734} = 1.5 \times 10^4 \text{M}^{-1} \text{cm}^{-1}$ (ref. 33).

for the reduction of $\text{ABTS}^{\bullet-}$ (i.e., Fig. 3-i). No degradation of $\text{ABTS}^{\bullet-}$ in PBS was observed after treatment with $5 \mu\text{M}$ **Ru1** (Fig. 3-ii), indicating this solution lacked a suitable terminal reductant. Subsequent addition of 50 mM EtOH to this PBS solution containing $5 \mu\text{M}$ **Ru1** and $50 \mu\text{M}$ $\text{ABTS}^{\bullet-}$ caused the $\text{ABTS}^{\bullet-}$ concentration to decrease (Fig. 3-iii), evidence that the electrons needed for the $\text{ABTS}^{\bullet-}$ reduction observed in Fig. 1 were ultimately supplied by the EtOH solvent.

If the hypothesis that the oxidation of $\text{R}_1\text{-CHOH-R}_2$ to $\text{R}_1\text{-C(=O)-R}_2$ provides the electrons necessary for the reduction of $\text{ABTS}^{\bullet-}$ to ABTS^{2-} is correct (i.e., Scheme 1-v), then both the O-H and C-H groups in a -CHOH- moiety will be essential for terminal reductant function. To test this hypothesis, PBS solutions containing $5 \mu\text{M}$ **Ru1** and $50 \mu\text{M}$ $\text{ABTS}^{\bullet-}$ were treated with 50 mM MeOH, i-PrOH, *t*-BuOH, ethylene glycol (EG) or 1,2-dimethoxyethane (DME) and the $\text{ABTS}^{\bullet-}$ concentration was measured. With MeOH, i-PrOH and EG, the $\text{ABTS}^{\bullet-}$ concentration began to decrease immediately following addition of the alcohol, indicating that these alcohols could serve as terminal reductants (Fig. S4–S6†). In contrast, no $\text{ABTS}^{\bullet-}$ reduction was

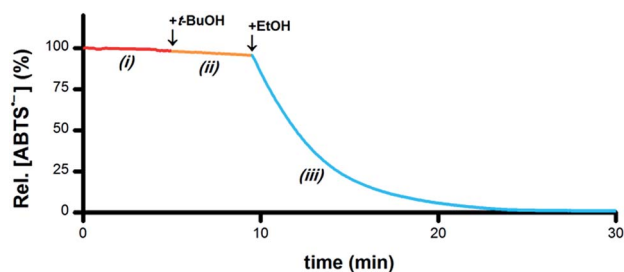


Fig. 4 Plot of relative $[\text{ABTS}^{\bullet-}]$ vs. time which shows the catalyst is not deactivated by *t*-BuOH. In a PBS solution containing only **Ru1**, $\text{ABTS}^{\bullet-}$ was stable (i, red line). Addition of *t*-BuOH did not cause any $\text{ABTS}^{\bullet-}$ reduction (ii, orange line). Subsequent addition of EtOH resulted in $\text{ABTS}^{\bullet-}$ degradation (iii, blue line), indicating that the lack of reactivity with *t*-BuOH was not due to catalyst deactivation. Conditions $[\text{Ru1}]_0 = 5 \mu\text{M}$, $[\text{ABTS}^{\bullet-}]_0 = 50 \mu\text{M}$, $[\text{t-BuOH}]_0 = 50 \text{mM}$, $[\text{EtOH}]_0 = 50 \text{mM}$, PBS (pH 7.4), 25°C ; $[\text{ABTS}^{\bullet-}]$ determined using absorbance measured at 734 nm and $\epsilon_{734} = 1.5 \times 10^4 \text{M}^{-1} \text{cm}^{-1}$ (ref. 33).

observed with DME or *t*-BuOH (e.g., Fig. 4-ii). However, when the addition of 50 mM *t*-BuOH was followed by 50 mM EtOH, $\text{ABTS}^{\bullet-}$ reduction did occur (Fig. 4-iii), revealing that the lack of reactivity with *t*-BuOH was not due to catalyst deactivation but rather the inability of *t*-BuOH to serve as a terminal reductant. Collectively, these results show that the C-H and O-H groups of a -CHOH- moiety are both essential for terminal reductant function, which is consistent with the hypothesis that oxidation of $\text{R}_1\text{-CHOH-R}_2$ to $\text{R}_1\text{-C(=O)-R}_2$ provides the reducing equivalents necessary to convert $\text{ABTS}^{\bullet-}$ to ABTS^{2-} . Replacing either the C-H group with C-Me or the O-H group with O-Me precludes this oxidation and thus the ability to function as a terminal reductant, which is supported by the lack of $\text{ABTS}^{\bullet-}$ reduction observed with *t*-BuOH and DME.

Biologically-relevant terminal reductants

A wide variety of biomolecules comprise -CHOH- groups, therefore we hypothesized that sugars, amino acids and citric acid cycle metabolites could serve as suitable terminal reductants in **Ru1**-catalyzed $\text{ABTS}^{\bullet-}$ reduction. To test this hypothesis, PBS solutions containing $5 \mu\text{M}$ **Ru1** and $50 \mu\text{M}$ $\text{ABTS}^{\bullet-}$ were treated with 50 mM serine, threonine, glucose, arabinose, malic acid or lactic acid. Reduction of $\text{ABTS}^{\bullet-}$ was markedly slower following the addition of the amino acids compared to the sugars, consistent with the greater number of CH-OH groups per molecule in the latter (Fig. 5). No significant differences in reactivity were observed between serine and threonine or between glucose and arabinose.

Malic acid and lactic acid are metabolites of the citric acid cycle and each comprises a -CHOH- group. However, no $\text{ABTS}^{\bullet-}$ reduction occurred following the addition of 50 mM malic acid or lactic acid to $5 \mu\text{M}$ **Ru1** and $50 \mu\text{M}$ $\text{ABTS}^{\bullet-}$ in PBS (Fig. 6). Malate and lactate will be the predominant species in pH 7.4 PBS, and these carboxylate anions can function as chelating bidentate ligands, which could potentially disrupt the catalytic activity of **Ru1**. To prevent catalyst deactivation, the methyl esters of these substrates were used. Addition of 50 mM methyl lactate (Me-lactate) or dimethyl malate (Me_2 -malate) to PBS solutions containing $5 \mu\text{M}$ **Ru1** and $50 \mu\text{M}$ $\text{ABTS}^{\bullet-}$ caused the $\text{ABTS}^{\bullet-}$ concentration to decrease rapidly. None of the biologically-relevant alcohols afforded $\text{ABTS}^{\bullet-}$ reduction in the

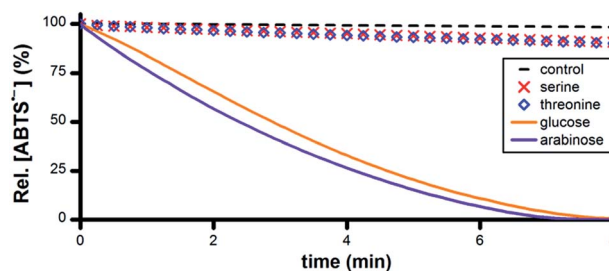


Fig. 5 Plot of relative $[\text{ABTS}^{\bullet-}]$ vs. time following the addition of amino acid or sugar ($t = 0$) to PBS solutions containing $\text{ABTS}^{\bullet-}$ and **Ru1**. Conditions: $[\text{Ru1}]_0 = 5 \mu\text{M}$, $[\text{ABTS}^{\bullet-}]_0 = 50 \mu\text{M}$, $[\text{ROH}]_0 = 50 \text{mM}$, PBS (pH 7.4), 25°C ; $[\text{ABTS}^{\bullet-}]$ determined using absorbance measured at 734 nm and $\epsilon_{734} = 1.5 \times 10^4 \text{M}^{-1} \text{cm}^{-1}$ (ref. 33).



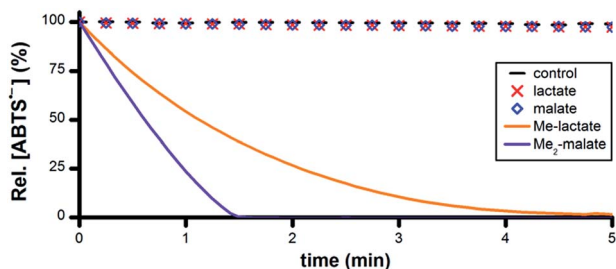


Fig. 6 Plot of relative $[\text{ABTS}^{\bullet-}]$ vs. time following the addition of lactate, malate or their methyl esters ($t = 0$) to PBS solutions containing $\text{ABTS}^{\bullet-}$ and Ru1 . Conditions: $[\text{Ru1}]_0 = 5 \mu\text{M}$, $[\text{ABTS}^{\bullet-}]_0 = 50 \mu\text{M}$, $[\text{ROH}]_0 = 50 \text{mM}$, PBS (pH 7.4), 25°C ; $[\text{ABTS}^{\bullet-}]$ determined using absorbance measured at 734nm and $\epsilon_{734} = 1.5 \times 10^4 \text{M}^{-1} \text{cm}^{-1}$ (ref. 33).

absence of Ru1 , and no oxidation of ABTS^{2-} to $\text{ABTS}^{\bullet-}$ by Ru1 was observed under any experimental conditions in PBS.

Inhibition of oxidative radical formation

Having obtained unambiguous evidence that Ru1 catalyzes $\text{ABTS}^{\bullet-}$ reduction using biologically-relevant alcohols as terminal reductants, we next sought to demonstrate that Ru1 could also inhibit radical formation. As the model system, we utilized the *in situ* oxidation of ABTS^{2-} to $\text{ABTS}^{\bullet-}$ by horseradish peroxidase (HRP) and H_2O_2 (*i.e.*, Scheme 1-ii).³⁹ Addition of $10 \mu\text{M}$ H_2O_2 to a PBS solution of 10nM HRP, $20 \mu\text{M}$ ABTS^{2-} , $5 \mu\text{M}$ Ru1 , and 50mM EtOH caused the $\text{ABTS}^{\bullet-}$ concentration to increase immediately. The $\text{ABTS}^{\bullet-}$ concentration peaked at $1.0 \mu\text{M}$ after 2.3min , which then gradually declined and complete $\text{ABTS}^{\bullet-}$ reduction was observed 13min after the peak (Fig. 7A, red line). No $\text{ABTS}^{\bullet-}$ formation occurred when $10 \mu\text{M}$ H_2O_2 was added to $5 \mu\text{M}$ Ru1 and $20 \mu\text{M}$ ABTS^{2-} in PBS, indicating that Ru1 did not cause any pro-oxidant reactions. Because Ru1 and Trolox were added as $30 \mu\text{L}$ aliquots from 5.0mM stock solutions in CH_3CN , $10 \mu\text{M}$ H_2O_2 was added to a PBS solution containing 10nM HRP, $20 \mu\text{M}$ ABTS^{2-} and 0.19M CH_3CN for the influence of this solvent. The radical absorbance immediately began to increase and reached a maximum of $17.9 \mu\text{M}$ after 50min (Fig. 7A, dotted green line and Fig. S7†). In contrast, the addition

of $10 \mu\text{M}$ H_2O_2 to a PBS solution of $5 \mu\text{M}$ Trolox, 10nM HRP and $20 \mu\text{M}$ ABTS^{2-} resulted in no change in $\text{ABTS}^{\bullet-}$ concentration for the first 7.6min , demonstrating that Trolox completely halted $\text{ABTS}^{\bullet-}$ formation (Fig. 7A, blue line). After 7.6min , however, the $\text{ABTS}^{\bullet-}$ concentration began to increase and reached a maximum of $9.3 \mu\text{M}$ at 12min after the onset of $\text{ABTS}^{\bullet-}$ formation. Notably, the maximum $[\text{ABTS}^{\bullet-}]$ observed in the presence of Trolox was $8.6 \mu\text{M}$ lower than the control, which was consistent with the ability of Trolox to function as a $2e^-$ reductant (*cf.*, the 22% decrease observed with Trolox in Fig. 1A). For the control and Trolox experiments, the decline in $\text{ABTS}^{\bullet-}$ concentration after peaking was consistent with normal $\text{ABTS}^{\bullet-}$ thermal decay.

To determine if Ru1 remained catalytically competent after the complete reduction of $\text{ABTS}^{\bullet-}$ formed by 10nM HRP and $10 \mu\text{M}$ H_2O_2 , two additional $10 \mu\text{M}$ aliquots of H_2O_2 were introduced (Fig. 7B, red line). Impressively, the concentration of $\text{ABTS}^{\bullet-}$ never exceeded $0.4 \mu\text{M}$ and decreased back to zero in less than 16min after the introduction of the second and third H_2O_2 aliquots. In contrast, addition of the second $10 \mu\text{M}$ H_2O_2 aliquot to the Trolox experiment caused the $\text{ABTS}^{\bullet-}$ concentration to gradually increase by $7.9 \mu\text{M}$ over the course of 38min (Fig. 7B, blue line), effectively resulting in complete oxidation of ABTS^{2-} to $\text{ABTS}^{\bullet-}$ (96% of the $17.9 \mu\text{M}$ observed for control). It was therefore unsurprising that the third $10 \mu\text{M}$ H_2O_2 aliquot produced no change in radical absorbance. Subsequent addition of 50mM EtOH and $5 \mu\text{M}$ Ru1 caused the $\text{ABTS}^{\bullet-}$ concentration to decrease rapidly, affording quantitative $\text{ABTS}^{\bullet-}$ reduction in less than 30min .

To confirm that the results obtained with Ru1 arose from its ability to catalyze $\text{ABTS}^{\bullet-}$ reduction, rather than inhibiting HRP or another chemical reaction, two $10 \mu\text{M}$ aliquots of chemically synthesized $\text{ABTS}^{\bullet-}$ were introduced after the $\text{ABTS}^{\bullet-}$ concentration had decreased to zero following the initial addition of $10 \mu\text{M}$ H_2O_2 (Fig. 7C, red line). The first and second $\text{ABTS}^{\bullet-}$ aliquots produced immediate increases in $\text{ABTS}^{\bullet-}$ concentration corresponding to 6.3 and $6.7 \mu\text{M}$, respectively, followed by rapid decreases in radical absorbance that resulted in quantitative radical reduction within 75s of aliquot addition. With the Trolox experiment, however, the first and second $\text{ABTS}^{\bullet-}$ aliquots caused $[\text{ABTS}^{\bullet-}]$ to increase by 9.9 and $9.7 \mu\text{M}$, respectively, with

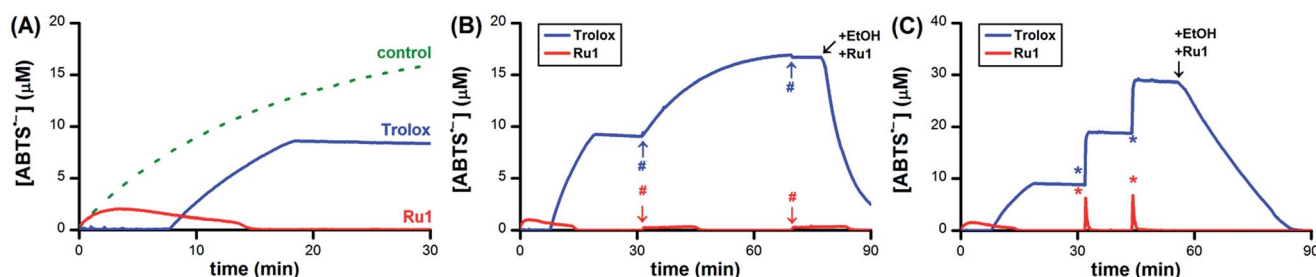


Fig. 7 (A) Plot of relative $[\text{ABTS}^{\bullet-}]$ vs. time which shows the *in situ* oxidation of ABTS^{2-} to $\text{ABTS}^{\bullet-}$ via HRP and H_2O_2 in the presence of Ru1 and EtOH (red line), Trolox (blue line) or 0.19M CH_3CN as a control (dotted green line). Plot of relative $[\text{ABTS}^{\bullet-}]$ vs. time which shows the (B) $\text{ABTS}^{\bullet-}$ formation by HRP in the presence of Ru1 and EtOH (red line) or Trolox (blue line) followed by two additional aliquots of $10 \mu\text{M}$ H_2O_2 (#) or (C) two $10 \mu\text{M}$ aliquots of chemically synthesized $\text{ABTS}^{\bullet-}$ (*). For the Trolox experiments shown in (B) or (C), 50mM EtOH and $5 \mu\text{M}$ Ru1 were added after the final aliquot of H_2O_2 or $\text{ABTS}^{\bullet-}$, respectively. Conditions: $[\text{HRP}]_0 = 10 \text{nM}$, $[\text{Ru1}]_0$ or $[\text{Trolox}]_0 = 5 \mu\text{M}$, $[\text{H}_2\text{O}_2]_0 = 10 \mu\text{M}$, $[\text{ABTS}^{2-}]_0 = 20 \mu\text{M}$, $[\text{EtOH}]_0 = 50 \text{mM}$, PBS (pH 7.4) at 25°C ; $[\text{ABTS}^{\bullet-}]$ determined using absorbance measured at 734nm and $\epsilon_{734} = 1.5 \times 10^4 \text{M}^{-1} \text{cm}^{-1}$ (ref. 33).



no observable changes in radical absorbance other than thermal decay (Fig. 7C, blue line). Addition of 50 mM EtOH and 5 μM **Ru1** after the second ABTS $^{\cdot-}$ aliquot afforded complete ABTS $^{\cdot-}$ reduction within 30 min, similar to the experiment with multiple H₂O₂ aliquots. Both AscH $^-$ and GSH inhibited the HRP-induced oxidation of ABTS $^{2-}$, albeit for shorter periods of time and less effectively than Trolox. The introduction of additional H₂O₂ (Fig. S8 and S9 \dagger) or ABTS $^{\cdot-}$ aliquots (Fig. S10 and S11 \dagger) only afforded increases in ABTS $^{\cdot-}$ concentration that mirrored the behaviors observed for Trolox (*i.e.*, Fig. 7B and C). Subsequent addition of 50 mM EtOH and 5 μM **Ru1** to the AscH $^-$ and GSH solutions containing excess ABTS $^{\cdot-}$ produced quantitative radical reduction, consistent with the Trolox experiments.

Conclusions

An organoruthenium complex (**Ru1**) that was previously reported to catalyze the hydrogenation of unsaturated organic substrates, using the oxidation of *i*-PrOH to acetone to supply the needed H₂, has now been shown to also catalyze the reduction of ABTS $^{\cdot-}$ to ABTS $^{2-}$ in buffered aqueous solution. By itself, **Ru1** was unreactive towards ABTS $^{\cdot-}$ and the presence of a non-tertiary alcohol was essential for ABTS $^{\cdot-}$ reduction to occur. Replacing either the C-H or O-H group in a -CHOH- moiety with C-Me or O-Me, respectively, resulted in the loss of ABTS $^{\cdot-}$ reducing ability. Given the previously reported transfer hydrogenation activity of **Ru1** and the fact that **Ru1**-catalyzed ABTS $^{\cdot-}$ reduction required a reactant comprising a -CHOH- moiety, we deduced that the reducing equivalents necessary for the 1e $^-$ reduction of ABTS $^{\cdot-}$ to ABTS $^{2-}$ were supplied by the oxidation of R₁-CHOH-R₂ to R₁-C(=O)-R₂. Consistent with this deduction, a diverse array of biologically-relevant non-tertiary alcohols, including amino acids, sugars and citric acid cycle metabolites, were found to be suitable terminal reductants for the reduction of ABTS $^{\cdot-}$ catalyzed by **Ru1**. Furthermore, in conjunction with an alcohol terminal reductant, **Ru1** was able to inhibit the oxidation of ABTS $^{2-}$ to ABTS $^{\cdot-}$ by H₂O₂ and horseradish peroxidase. In contrast, non-catalytic antioxidants (Trolox, ascorbate, glutathione), only offered limited protection that, once exhausted, had no impact on ABTS $^{\cdot-}$ formation or stability. Impressively, no ABTS $^{\cdot-}$ formation or other pro-oxidant effects by **Ru1** were observed under any experimental conditions. The mechanism for the catalytic reduction of ABTS $^{\cdot-}$ by **Ru1** and non-tertiary alcohols, along with the biological applications, will be detailed in subsequent reports.

Acknowledgements

We are grateful to A. Mangalum for preceding work and helpful insight into the synthesis of **2** and **Ru1**.

Notes and references

\dagger In PBS, an ABTS $^{\cdot-}$ concentration of 6.7 μM would give rise to an absorbance value of 0.1. Achieving a similar value with O₂ $^{\cdot-}$ or H₂O₂ would require a concentration of 53 μM or 2.29 mM, respectively.

\S The concentration of the successive ABTS $^{\cdot-}$ aliquots was selected based on the concentration of the initial 50 μM ABTS $^{\cdot-}$ that was degraded by the antioxidant. Because **Ru1** degraded all of the initial 50 μM ABTS $^{\cdot-}$ and Trolox only degraded 10 μM , the concentration of the multiple sequential aliquots added was 50 μM with **Ru1** and 10 μM with Trolox.

- 1 M. P. Murphy, *Biochem. J.*, 2009, **417**, 1–13.
- 2 M. Valko, D. Leibfritz, J. Moncol, M. T. D. Cronin, M. Mazur and J. Telser, *Int. J. Biochem. Cell Biol.*, 2007, **39**, 44–84.
- 3 M. S. Cooke, M. D. Evans, M. Dizdaroglu and J. Lunec, *FASEB J.*, 2003, **17**, 1195–1214.
- 4 W. Maret, *Antioxid. Redox Signaling*, 2006, **8**, 1419–1441.
- 5 R. Stocker and J. F. Keaney Jr, *Physiol. Rev.*, 2004, **84**, 1381–1478.
- 6 T. Fukai and M. Ushio-Fukai, *Antioxid. Redox Signaling*, 2011, **15**, 1583–1606.
- 7 S. Miriyala, I. Spasojevic, A. Tovmasyan, D. Salvemini, Z. Vujaskovic, D. S. Clair and I. Batinic-Haberle, *Biochim. Biophys. Acta*, 2012, **1822**, 794–814.
- 8 I. Batinic-Haberle, A. Tovmasyan, E. R. H. Roberts, Z. Vujaskovic, K. W. Leong and I. Spasojevic, *Antioxid. Redox Signaling*, 2014, **20**, 2372–2415.
- 9 S. D. Amaral and B. P. Espósito, *Biomaterials*, 2008, **21**, 425–432.
- 10 M. K. Evans, A. Tovmasyan, I. Batinic-Haberle and G. R. Devi, *Free Radical Biol. Med.*, 2014, **68**, 302–314.
- 11 P. Chelikani, I. Fita and P. C. Loewen, *Cell. Mol. Life Sci.*, 2004, **61**, 192–208.
- 12 H.-P. Hersleth, U. Ryde, P. Rydberg, C. H. Görbitz and K. K. Andersson, *J. Inorg. Biochem.*, 2006, **100**, 460–476.
- 13 H. N. Kirkman and G. F. Gaetani, *Trends Biochem. Sci.*, 2007, **32**, 44–50.
- 14 J. Vlasits, C. Jakopitsch, M. Bernroither, M. Zamocky, P. G. Furtmüller and C. Obinger, *Arch. Biochem. Biophys.*, 2010, **500**, 74–81.
- 15 R. Kubota, S. Imamura, T. Shimizu, S. Asayama and H. Kawakami, *ACS Med. Chem. Lett.*, 2014, **5**, 639–643.
- 16 M. A. Sharpe, R. Olloson, V. C. Stewart and J. B. Clark, *Biochem. J.*, 2002, **366**, 97–107.
- 17 M. Itoh, K.-i. Motoda, K. Shindo, T. Kamiyuki, H. Sakiyama, N. Matsumoto and H. Ōkawa, *J. Chem. Soc., Dalton Trans.*, 1995, 3635–3641.
- 18 Y. Naruta and K. Maruyama, *J. Am. Chem. Soc.*, 1991, **113**, 3595–3596.
- 19 R. A. Sheldon, *Catal. Today*, 2015, **247**, 4–13.
- 20 B. L. Ryland and S. S. Stahl, *Angew. Chem., Int. Ed.*, 2014, **53**, 8824–8838.
- 21 Y. Seki, K. Oisaki and M. Kanai, *Tetrahedron Lett.*, 2014, **55**, 3738–3746.
- 22 C. Parmeggiani and F. Cardona, *Green Chem.*, 2012, **14**, 547–564.
- 23 M. J. Schultz and M. S. Sigman, *Tetrahedron*, 2006, **62**, 8227–8241.
- 24 J. J. Soldevila-Barreda, I. Romero-Canelón, A. Habtemariam and P. J. Sadler, *Nat. Commun.*, 2015, **6**, 6582.
- 25 Y. Fu, M. J. Romero, A. Habtemariam, M. E. Snowden, L. Song, G. J. Clarkson, B. Qamar, A. M. Pizarro, P. R. Unwin and P. J. Sadler, *Chem. Sci.*, 2012, **3**, 2485–2494.



- 26 J. J. Soldevila-Barreda and P. J. Sadler, *Curr. Opin. Chem. Biol.*, 2015, **25**, 172–183.
- 27 P. K. Sasmal, C. N. Streu and E. Meggers, *Chem. Commun.*, 2013, **49**, 1581–1587.
- 28 G. Gasser and N. Metzler-Nolte, *Curr. Opin. Chem. Biol.*, 2012, **16**, 84–91.
- 29 A. Mangalum, C. D. McMillen and A. G. Tennyson, *Inorg. Chim. Acta*, 2015, **426**, 29–38.
- 30 S. P. Fricker, E. Slade, N. A. Powell, O. J. Vaughan, G. R. Henderson, B. A. Murrer, I. L. Megson, S. K. Bisland and F. W. Flitney, *Br. J. Pharmacol.*, 1997, **122**, 1441–1449.
- 31 B. R. Cameron, M. C. Darkes, H. Yee, M. Olsen, S. P. Fricker, R. T. Skerlj, G. J. Bridger, N. A. Davies, M. T. Wilson, D. J. Rose and J. Zubieta, *Inorg. Chem.*, 2003, **42**, 1868–1876.
- 32 A. Mangalum, Y. Htet, D. A. Roe, C. D. McMillen and A. G. Tennyson, *Inorg. Chim. Acta*, 2015, **435**, 320–326.
- 33 R. Re, N. Pellegrini, A. Proteggente, A. Pannala, M. Yang and C. Rice-Evans, *Free Radical Biol. Med.*, 1999, **26**, 1231–1237.
- 34 U. Jungwirth, C. R. Kowol, B. K. Keppler, C. G. Hartinger, W. Berger and P. Heffeter, *Antioxid. Redox Signaling*, 2011, **15**, 1085–1127.
- 35 B. H. J. Bielski and A. O. Allen, *J. Phys. Chem.*, 1977, **81**, 1048–1050.
- 36 K. Yusa and K. Shikama, *Biochemistry*, 1987, **26**, 6684–6688.
- 37 D. Huang, B. Ou and R. L. Prior, *J. Agric. Food Chem.*, 2005, **53**, 1841–1856.
- 38 M. Karbarz and J. Malyszko, *Electroanalysis*, 2008, **20**, 1884–1890.
- 39 L. Pitulice, I. Pastor, E. Vilaseca, S. Madurga, A. Isvoran, M. Cascante and F. Mas, *Biocatal. Biotransform.*, 2013, **2**, 1–5.
- 40 C. Creutz, *Inorg. Chem.*, 1981, **20**, 4449–4452.
- 41 J. M. Pullar, M. C. M. Vissers and C. C. Winterbourn, *J. Biol. Chem.*, 2001, **276**, 22120–22125.
- 42 S. Enami, M. R. Hoffmann and A. J. Colussi, *Chem. Res. Toxicol.*, 2009, **22**, 35–40.
- 43 P. Sathyadevi, P. Krishnamoorthy, N. S. P. Bhuvanesh, P. Kalaiselvi, V. V. Padma and N. Dharmaraj, *Eur. J. Med. Chem.*, 2012, **55**, 420–431.
- 44 Y. Liu, X. Zhang, R. Zhang, T. Chen, Y.-S. Wong, J. Liu and W.-J. Zheng, *Eur. J. Inorg. Chem.*, 2011, 1974–1980.
- 45 J. M. Alfaro, A. Prades, M. del Carmen Ramos, E. Peris, J. Ripoll-Gómez, M. Poyatos and J. S. Burgos, *Zebrafish*, 2010, **7**, 13–21.

